TOWARDS THREE-DIMENSIONAL ACTIVE INCOHERENT MILLIMETER-WAVE IMAGING

Stavros Vakalis and Jeffrey A. Nanzer

Electrical and Computer Engineering, Michigan State University

ABSTRACT

Active incoherent millimeter-wave (AIM) imaging is a new technique that combines aspects of passive millimeter-wave imaging and noise radar to obtain high-speed imagery. Using an interferometric receiving array combined with small set of uncorrelated noise transmitters, measurements of the Fourier transform domain of the scene can be rapidly obtained, and scene images can be generated quickly via two-dimensional inverse Fourier transform. Previously, AIM imaging provided two-dimensional reconstructions of the scene. In this work we explore the use of active millimeter-wave imaging for automotive sensing by investigating array feasible layouts for automobiles, and a new technique to impart range estimation to obtain three-dimensional imaging information.

Index Terms— Millimeter-wave imaging, high-speed imaging, noise radar, automotive radar

1. INTRODUCTION

Millimeter-wave imaging has benefits for a wide range of applications, including security sensing [1], contraband detection [2], medical imaging [3], and non-destructive testing [4], among others. Recently, millimeter-wave imaging for automotive radar has become of significant interest due to the rapidly evolving field of vehicle autonomy [5, 6, 7, 8]. Millimeter-wave imaging holds significant potential for automotive applications due to the ability of millimeter-wave radiation to propagate through obscurants like fog, smoke, snow, and light rain with little to no impact, while at the same time maintaining good imaging resolution due to the short wavelengths of millimeter-wave signals [1].

Millimeter-wave automotive sensing uses active transmission of signals, rather than passive techniques, to ensure sufficient sensing range and operational speed. Active imaging at millimeter-wave frequencies traditionally relies on the transmission and reception of a coherent radar signal combined with a narrow beam steered either mechanically or electrically [9]. Mechanical imagers tend to be bulky and slow [10], limiting their feasibility in automotive applications, while electrically-scanned systems require a significant number of

electrical components and a large aperture to generate highresolution imagery, driving up cost and power consumption. Multiple-input and multiple-output (MIMO) techniques combined with frequency-modulated continuous-wave (FMCW) radar waveforms can achieve imaging without analog beamforming [11], however MIMO FMCW radar systems require complex synchronization between the receive and transmit array elements, and also entail a significant amount of additional processing since each transmit signal is processed orthogonally on each receiving element [12].

In this work we introduce a new concept for three-dimensional automotive sensing that builds on a recently developed active incoherent millimeter-wave (AIM) imaging technique. In contrast to traditional millimeter-wave techniques, AIM imaging combines the transmission of noise signals with a sparse interferometric receiving aperture to obtain high-resolution two-dimensional millimeter-wave imagery at video rates, without scanning [13, 14]. Here we explore a new concept that imparts a coarse time synchronization of the transmitted noise waveforms to obtain range resolution and thus imaging in three dimensions. We investigate two array layouts commensurate with implementation on a vehicle facade at 77 GHz and investigate the three-dimensional response of the system with a wideband pulsed noise waveform.

2. ACTIVE INCOHERENT MILLIMETER-WAVE (AIM) IMAGING

Interferometric imaging was first developed in radio astronomy to observe the radiation from stars and other stellar objects using sparse arrays to sample the spatial Fourier transform of the signals in the array field of view [15], but has since been applied to satellite remote sensing and security sensing. Interferometric arrays sample the Fourier transform of the scene intensity, instead of sampling the scene intensity directly like other imaging modalities. Interferometric imaging systems can use sparse antenna arrays requiring significantly fewer antenna elements than traditional phased arrays, while also maintaining a tolerance to element failures [16, 17]. Interferometric arrays have traditionally been passive systems, capturing thermal emissions from the scene. Interferometric imaging necessitates that the received signals are spatially

This work was supported by the National Science Foundation under Grant 1708820.

and temporally incoherent to reconstruct the scene from the Fourier domain samples [15], and thermal radiation naturally satisfies this constraint. However, thermal radiation power is generally exceedingly small at millimeter-wave frequencies, requiring highly sensitive receivers with high gain and long integration times, limiting the practicability of the technique for automotive applications, where fast image reconstruction time and low cost is important.

In AIM imaging, we combine the benefits of active and passive millimeter-wave imaging. Active millimeter-wave systems operate with significantly higher signal-to-noise ratio (SNR) due to the transmission of signals, and therefore do not require receivers with high sensitivity. Passive interferometric millimeter-wave systems employ very sparse antenna arrays and, furthermore, generate imagery in a staring format, without beamsteering. We previously demonstrated AIM imaging at microwave and millimeter-wave frequencies using multiple noise transmitters to effectively mimic the properties of thermal radiation and support Fourier-domain image reconstruction [13, 14].

Interferometric antenna arrays, whether used for passive or AIM imaging, capture samples of the scene visibility $\mathcal{V}(u,v)$, which is the spatial Fourier transform of the scene where (u,v) are spatial frequencies. Samples of the visibility are obtained via cross-correlation of the signals between pairs of antennas, yielding a sampling function S(u,v), where the sampled spatial frequencies are defined by the electrical separation and rotation angle of the antenna pairs. The product of the sampling function S(u,v) and $\mathcal{V}(u,v)$ is referred to as the sampled visibility $\mathcal{V}_s(u,v)$, from which the image intensity I_r can be reconstructed through an inverse Fourier transform

$$I_r(\alpha, \beta) = \iint_{-\infty}^{\infty} \mathcal{V}_s(u, v) e^{-j2\pi(u\alpha + v\beta)} du dv \qquad (1)$$

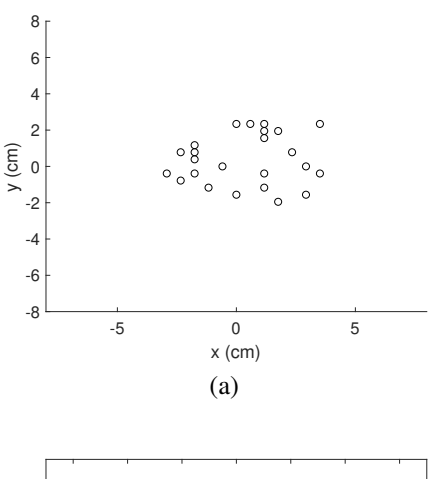
where α and β are the direction cosines in the azimuth and elevation plane. The spatial response of an interferometric array can be characterized by the point spread function, which is given by

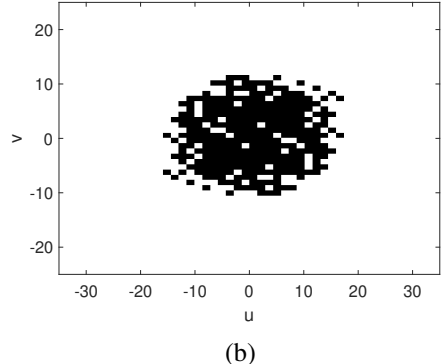
$$PSF = \mathcal{F}^{-1} \Big[S(u, v) \Big]. \tag{2}$$

In incoherent imaging the point spread function typically refers to the squared magnitude $|PSF|^2$.

3. ANALYSIS OF AIM IMAGING FOR 77 GHZ AUTOMOTIVE RADAR

We consider the imaging performance of two 24-element 77 GHz array layouts for potential implementation in the facade of a vehicle: a randomized aperture that has the same azimuth and elevation resolution and a randomized aperture using the same number of elements that increases resolution in the azimuth plane at the expense of resolution in the elevation plane. Wider inter-element spacing can lead to larger





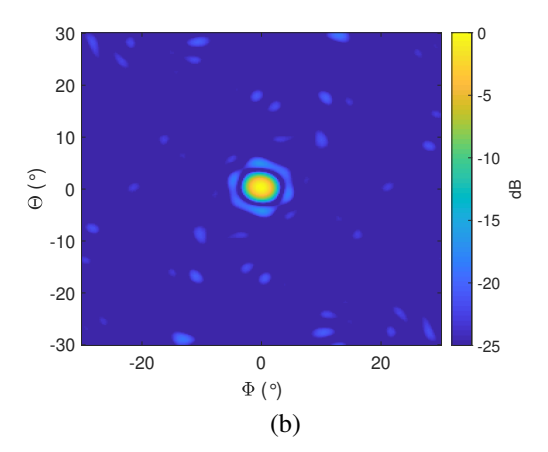


Fig. 1. (a) Randomized 24-element antenna array. The minimum spacing in both the horizontal and vertical dimension is 1.5 λ . (b) Sampling function of the random 24-element aperture. (c) Point spread function of the randomized aperture as a function of the azimuth and elevation angles Φ and Θ .

electrical aperture maximum dimensions, and therefore improved resolution, however this also introduces image ambiguities, limiting the effective field-of-view of the imager. The half-angle unambiguous field of view of an interferometric imager with element spacing d_x and d_y across the horizon-

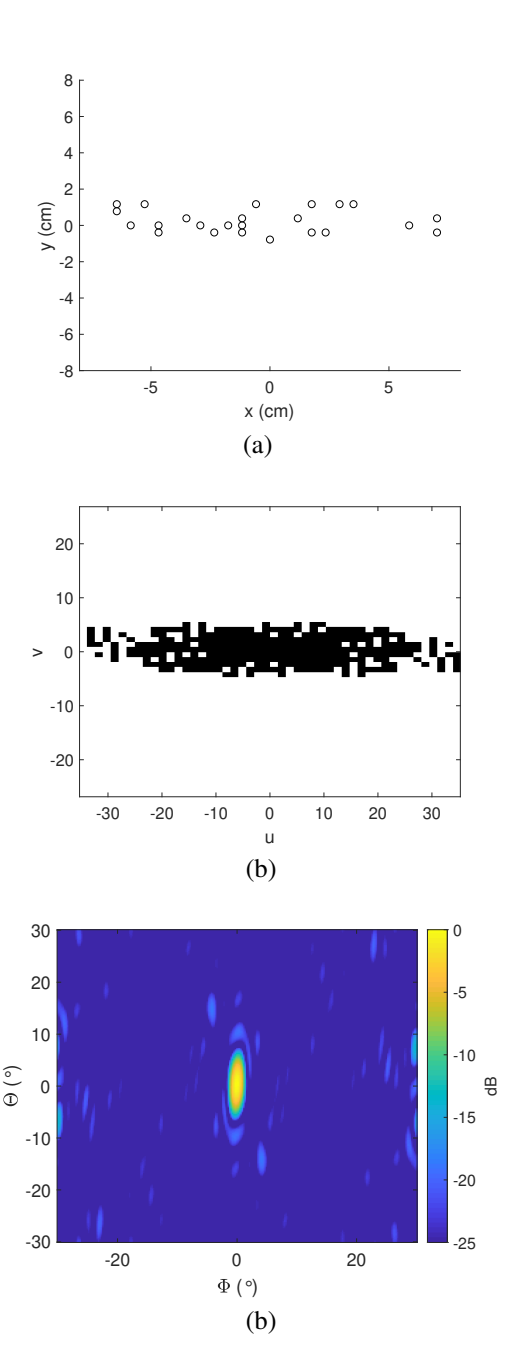


Fig. 2. (a) Random 24-element antenna array. The minimum spacing in both the horizontal and vertical dimension is 1.5 λ . (b) Sampling function of the random 24-element aperture. The sampling function is significantly wider in the u dimension. (c) Point spread function of the randomized aperture as a function of the azimuth and elevation angles Φ and Θ . The beamwidth is significantly larger in the elevation plane than in the azimuth plane, due to the smaller aperture electrical dimensions.

tal and vertical axes can be expressed for the two direction cosines α and β as

$$FOV_{\frac{\alpha}{2},\frac{\beta}{2}} = \frac{\lambda}{2 \cdot d_{x,y}} \quad . \tag{3}$$

The 24-element randomized antenna array with equal azimuth and elevation resolution is shown in Fig. 1(a). The minimum spacing between two antenna elements is 0.58 cm (1.5λ) , which corresponds to an ambiguous field of view of approximately $\pm 34^{\circ}$ in the azimuth (Φ) and elevation (Θ) angles. Due to its less stringent layout, random arrays allow more flexibility for integration into different vehicle facades. The sampling function S(u, v) of the array is shown in 1(b). The PSF of the array is shown in 1(c), which shows a resolution of 7 degrees in both azimuth and elevation dimensions. At a distance of 20 m from the aperture, the resolution is 2.42 m in the azimuth (cross-range) dimension. While this array has equivalent elevation and azimuth resolution, for automotive applications azimuth resolution is generally more important, thus we designed a second randomized aperture using the same number of elements, but spanning a wider horizontal space and a narrower vertical space. Since the resolution is inversely proportional to the maximum aperture size, this serves to improve the resolution in the azimuth dimension at the expense of resolution in the elevation dimension. In this case, the array was four times wider in the horizontal dimension that the vertical dimension. The second randomized 24element antenna array with 1.5λ minimum spacing in both the x and y dimension is shown in Fig. 2(a). The sampling function S(u, v) of the array is shown in 2(b). The point spread function can be seen in Fig. 2(c). The array maximum vertical dimension has decreased in this array, and therefore the resolution has become larger in the elevation plane and equal with 15 degrees, however the resolution has improved in the azimuth plane to 3.3 degrees, which is of greater importance. At a distance of 20 m from the aperture, the resolution is 1.16 m in the azimuth (cross-range) dimension. Apertures with wider horizontal coverage or more antenna elements could easily be designed to further improve the resolution.

4. 3-D AIM IMAGING

Interferometric imaging, both passive and active, do not inherently provide for a mechanism to obtain range information. For automotive applications, down-range measurements should generally be combined with cross-range measurements for accurate environmental sensing. Techniques using volumetric arrays or near-field processing have been explored [18, 19], however their requirements are not practical for automotive applications. Traditional coherent processing techniques, such as matched filtering, are not possible in passive interferometry since no transmit signal is used. In AIM, the specifics of the transmit signals need not be known to simplify the hardware requirements; simple noise emitters

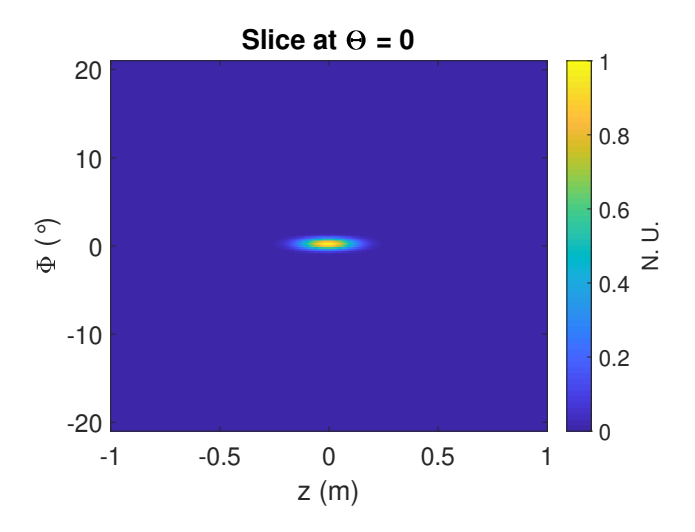


Fig. 3. Two-dimensional $\Phi-z$ slice of the $PSF(\Phi,\Theta,z)$ from the randomized aperture in Fig. 2(a). The bandwidth of the pulse is 200 MHz.

can be used as long as their statistics are known, precluding matched filtering.

In this work we explore a new approach of pulse modulating the transmitted noise signals to obtain down-range information. We control the timing of the transmitted signal envelopes, which can be done with relatively simple coordination and does not impose spatial coherence, thereby preserving the cross-range incoherence. The result effectively generates two-dimensional interferometric images sequentially in time, each time segment representing a different range bin. We analyze the PSF of the system using a Gaussian pulse on the transmitted noise signals. The frequency-domain signal on each transmitter can be written as

$$S_i(f) = e^{\frac{-(f - f_c)^2}{4\delta f^2}} N_i(f)$$
 (4)

where $N_i(f)$ is the spectrum of the ith wideband Gaussian noise signal, f_c is the carrier frequency and δf is the pulse bandwidth. The range resolution Δz along the z dimension can be approximated by the full width at half maximum of a squared Gaussian pulse as

$$\Delta z \approx \frac{2.3548 \, c}{\sqrt{2}\pi \delta f}.\tag{5}$$

For $\delta f=200$ MHz, $\Delta z\approx 20$ cm. For the three-dimensional simulations we assume that the carrier frequency of the imaging system is 77 GHz and the bandwidth δf is 200 MHz. A slice $\Phi-z$ of the point spread function $PSF(\Phi,\Theta,z)$ for the random array is shown in Fig. 3, demonstrating the downrange and cross-range resolution capabilities.

5. CONCLUSION

We investigated the point spread function of a new approach to achieve three-dimensional active incoherent millimeter-wave imaging. Array layouts were considered that matched automotive radar frequencies and physical sizes that are commensurate with potential application in an automotive facade. We investigated the use of pulse modulation on incoherent transmitted signals to add three-dimensional measurement capability to a previously demonstrated two-dimensional measurement system. Future efforts may build on this work to implement fast, robust environmental sensing for automotive applications.

6. REFERENCES

- [1] J. A. Nanzer, Microwave and Millimeter-Wave Remote Sensing for Security Applications, Artech House, 2012.
- [2] D. M. Sheen, D. L. McMakin, and T. E. Hall, "Three-dimensional millimeter-wave imaging for concealed weapon detection," *IEEE Trans. Microw. Theory Techn.*, vol. 49, no. 9, pp. 1581–1592, Sep 2001.
- [3] N. K. Nikolova, "Microwave imaging for breast cancer," *IEEE Microw. Mag.*, vol. 12, no. 7, pp. 78–94, Dec 2011.
- [4] F. Zidane, J. Lanteri, J. Marot, L. Brochier, N. Joachimowicz, H. Roussel, and C. Migliaccio, "Nondestructive control of fruit quality via millimeter waves and classification techniques: Investigations in the automated health monitoring of fruits," *IEEE Antennas Propag. Mag.*, vol. 62, no. 5, pp. 43–54, 2020.
- [5] Igal Bilik, Shahar Villeval, Daniel Brodeski, Haim Ringel, Oren Longman, Piyali Goswami, Chethan Y. B. Kumar, Sandeep Rao, Pramod Swami, Anshu Jain, Anil Kumar, Shankar Ram, Kedar Chitnis, Yashwant Dutt, Aish Dubey, and Stanley Liu, "Automotive multi-mode cascaded radar data processing embedded system," in 2018 IEEE Radar Conference (RadarConf18), 2018, pp. 0372–0376.
- [6] J. Hasch, E. Topak, R. Schnabel, T. Zwick, R. Weigel, and C. Waldschmidt, "Millimeter-wave technology for automotive radar sensors in the 77 ghz frequency band," *IEEE Trans. Microw. Theory Tech.*, vol. 60, no. 3, pp. 845–860, 2012.
- [7] J. Dickmann, J. Klappstein, M. Hahn, N. Appenrodt, H. Bloecher, K. Werber, and A. Sailer, "Automotive radar the key technology for autonomous driving: From detection and ranging to environmental understanding," in 2016 IEEE Radar Conference (RadarConf), 2016, pp. 1–6.

- [8] Martin Stolz, Mingkang Li, Zhaofei Feng, Martin Kunert, and Wolfgang Menzel, "High resolution automotive radar data clustering with novel cluster method," in 2018 IEEE Radar Conference (RadarConf18), 2018, pp. 0164–0168.
- [9] B. Ku, P. Schmalenberg, O. Inac, O. D. Gurbuz, J. S. Lee, K. Shiozaki, and G. M. Rebeiz, "A 77–81-ghz 16-element phased-array receiver with ±50° beam scanning for advanced automotive radars," *IEEE Trans. Microw. Theory Tech.*, vol. 62, no. 11, pp. 2823–2832, 2014.
- [10] Josiah Wayl Smith, Muhammet Emin Yanik, and Murat Torlak, "Near-field mimo-isar millimeter-wave imaging," in 2020 IEEE Radar Conference (RadarConf20), 2020, pp. 1–6.
- [11] R. Feger, C. Wagner, S. Schuster, S. Scheiblhofer, H. Jager, and A. Stelzer, "A 77-ghz fmcw mimo radar based on an sige single-chip transceiver," *IEEE Trans. Microw. Theory Tech.*, vol. 57, no. 5, pp. 1020–1035, May 2009.
- [12] Francesco Belfiori, Wim van Rossum, and Peter Hoogeboom, "Random transmission scheme approach for a fmcw tdma coherent mimo radar," in 2012 IEEE Radar Conference, 2012, pp. 0178–0183.
- [13] S. Vakalis and J. A. Nanzer, "Microwave imaging using noise signals," *IEEE Trans. Microw. Theory Techn.*, vol. 66, no. 12, pp. 5842–5851, Dec 2018.
- [14] S. Vakalis, L. Gong, Y. He, J. Papapolymerou, and J. A. Nanzer, "Experimental demonstration and calibration of a 16-element active incoherent millimeter-wave imaging array," *IEEE Trans. Microw. Theory Techn.*, vol. 68, no. 9, pp. 3804–3813, 2020.
- [15] A. R. Thompson, J. M. Moran, and G. W. Swenson, *Interferometry and Synthesis in Radio Astronomy*, John Wiley and Sons, 2001.
- [16] S. Vakalis and J. A. Nanzer, "Analysis of array sparsity in active incoherent microwave imaging," *IEEE Geosci. Remote Sens. Lett.*, vol. 17, no. 1, pp. 57–61, Jan 2020.
- [17] S. Vakalis and J. A. Nanzer, "Analysis of element failures in active incoherent microwave imaging arrays using noise signals," *IEEE Microw. Wireless Compon. Lett.*, vol. 29, no. 2, pp. 161–163, Feb 2019.
- [18] Joseph Rosen and Amnon Yariv, "Three-dimensional imaging of random radiation sources," *Opt. Lett.*, vol. 21, no. 14, pp. 1011–1013, Jul 1996.
- [19] N. A. Salmon, "3-d radiometric aperture synthesis imaging," *IEEE Trans. Microw. Theory Techn.*, vol. 63, no. 11, pp. 3579–3587, 2015.